

# Electrostatic Localized Structures in Collisionless Plasmas

SAEKI Koichi

*Department of Physics, Faculty of Science, Shizuoka University,  
Ohya 836, Shizuoka 422-8529, Japan*

(Received: 5 December 2000 / Accepted: 27 October 2001)

## Abstract

The relationship between a localized structure and a dispersion relation is investigated. The region of real phase velocity and imaginary wave number guarantees the existence of a sheath, a soliton and a phase-space hole, and suggests a new coupling state of an electron hole and an ion soliton (CHS). A computer simulation verifies that CHSs exist and propagate stably.

## Keywords:

localized structure, sheath, soliton, phase-space hole, coupled hole soliton, dispersion relation

## 1. Introduction

In plasmas, there exist various types of electrostatic localized structures: sheaths, solitons and phase-space holes etc. Sheaths and solitons are well known. Thus, we review simply phase-space holes (holes or phase-space vortices) [1]. Holes were found in computer runs simulating two stream instability [2]. Experimentally, an electron hole was discovered in a collisionless plasma of Q-machine [3]. The ion version of the hole was observed in DP-machine [4]. This ion hole has an important role on the anomalous electrical resistivity and the formation of ion acoustic double layers [5] and double layers [6]. On the other hand, the data of the spacecraft, GEOTAIL, recently revealed that most of the BEN (broad-band electrostatic noise) in the plasma of the geomagnetic tail is a series of electron holes [7].

These structures of sheaths, solitons and holes must be free of wave emission to maintain themselves. Accordingly, in chapter 2, we show the relationship between localized structures and dispersion relations. The tails of these localized structures are regarded as nonoscillatory and propagating evanescent waves with real phase velocity  $u$  and imaginary wave number  $k_i$  determined by the dispersion relation. In case of an unmagnetized plasma, ion holes belong to the region  $u <$

$\sqrt{3}v_{ti}$ . On the other hand, both electron holes and ion acoustic solitons belong to the region  $c_s < u < \sqrt{3}v_{te}$ . Thus, the dispersion suggests the existence of a coupled state of an electron hole and an ion acoustic soliton (abbreviated to a coupled hole-soliton or a CHS). Here,  $v_{ti}$ ,  $v_{te}$  and  $c_s$  are ion and electron thermal speeds and ion acoustic speed.

In chapter 3, we present experimental data of ion phase space holes. In chapter 4, the existence of a coupled hole soliton is revealed by a computer simulation and the theory of Saeki and Rasmussen [8].

## 2. Relationship between Localized Structures and Dispersion Relations

In plasmas, waves and nonlinear localized structures are important concepts, and are deeply related to dispersion relations. An ion acoustic soliton is one of typical electrostatic localized structures. Thus, we take up the dispersion relation of ion acoustic waves,

$$\varepsilon = \varepsilon_0 \left( 1 + \frac{k_{De}^2}{k^2} - \frac{\omega_{pe}^2}{k^2 u^2} \right) = 0. \quad (1)$$

and consider its relation to the ion acoustic soliton. Here,  $\varepsilon$ ,  $k_{De}$  and  $\omega_{pe}$  are plasma dielectric constant,

©2001 by The Japan Society of Plasma  
Science and Nuclear Fusion Research

\*Corresponding author's e-mail: spksaek@ipc.shizuoka.ac.jp

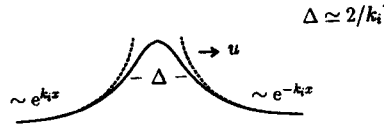
electron Debye wave number and ion plasma angular frequency, respectively. The relation between the phase velocity  $u$  and the wave number  $k$  is expressed schematically in Fig. 1. In the region that the phase velocity  $u$  is equal to or smaller than the ion acoustic speed  $c_s$ , the corresponding wave number is real, and normal ion acoustic waves propagate. On the other hand, the region of  $u > c_s$  gives pure imaginary wave numbers  $k_i$ ,

$$k_i = \sqrt{k_{De}^2 - \omega_{pi}^2/u^2} \approx k_{De} \sqrt{2(M-1)}, \quad (M-1 \ll 1) \quad (2)$$

and presents an ion acoustic soliton and an ion sheath. Here,  $M (= u/c_s)$  is Mach number. The tails of the ion soliton can be regarded as nonoscillatory and propagating evanescent waves being proportional to  $\exp(-k_i x)$  and  $\exp(-k_i x)$  on both sides. Thus, a dispersion relation determines the tail of a corresponding localized structure.

The form of an ion acoustic soliton is determined as follows. When we observe a soliton in the moving frame of the soliton speed  $u$ , the following conservation equations of ion energy and ion flux is maintained.

#### Ion Acoustic Soliton



#### Dispersion Relation

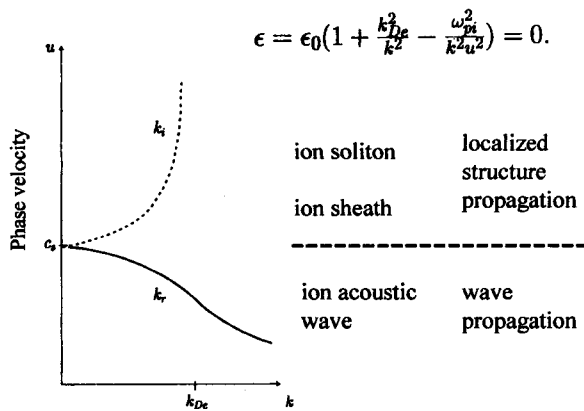


Fig. 1 Relation between an ion acoustic soliton and a dispersion relation. The imaginary wave number  $k_i$  derived from the dispersion relation determines its tail shape and its width  $\Delta$ .

$$\begin{aligned} \frac{1}{2} m_i (-u)^2 &= \frac{1}{2} m_i v_i^2(x) - e\phi(x), \\ n_0(-u) &= n_i(x) v_i(x). \end{aligned}$$

Here,  $m_i$ ,  $v_i$ ,  $\phi$ ,  $n_i$  and  $n_0$  are ion mass, ion velocity, soliton potential, ion density and equilibrium plasma density, respectively. In order to close the system describing the soliton, we need Boltzmann relation for electrons and Poisson's equation,

$$\begin{aligned} n_e(x) &= n_0 \exp \frac{e\phi(x)}{\kappa T_e}, \\ \frac{\partial^2 \phi(x)}{\partial x^2} &= \frac{e}{\epsilon_0} (n_e(x) - n_i(x)). \end{aligned}$$

Here,  $n_e$ ,  $\kappa$  and  $T_e$  are electron density, Boltzmann's constant and electron temperature, respectively. After the calculation based on the above equations, we obtain the following equation,

$$\frac{\partial^2 \Phi}{\partial z^2} = \exp \Phi - M(M^2 - 2\Phi)^{-1/2}.$$

Here, we normalize the quantities as  $z = k_{De} x$ , and  $\Phi = e\phi/\kappa T_e$ . By integrating the above equation multiplied by  $\partial\Phi/\partial z$  from  $-\infty$  to  $z$ , we derive Sagdeev's potential  $V(\Phi)$ ,

$$\begin{aligned} V(\Phi) &= 1 - \exp \Phi + M(M - (M^2 - 2\Phi)^{-1/2}), \\ &\approx -(M-1)\Phi^2 + \Phi^3/6, \quad (\Phi \ll 1) \end{aligned}$$

which satisfies  $(1/2)(\partial\Phi/\partial z)^2 + V(\Phi) = 0$ . The solution of a small-amplitude soliton is  $\Phi = 3(M-1) \operatorname{sech}^2 \sqrt{(M-1)/2} x$ . In laboratory frame,

$$\begin{aligned} \phi &= \phi_{\max} \operatorname{sech}^2 \left( \frac{x-ut}{\Delta} \right), \\ \frac{u-c_s}{c_s} &= \frac{2}{k_{De}^2 \Delta^2} = \frac{e\phi_{\max}}{3\kappa T_e}. \end{aligned}$$

Here,  $\phi_{\max}$  is the maximum potential of the soliton. Thus, the relation between the width of the soliton  $\Delta$  and the soliton velocity  $u$  is as follows.

$$\frac{2}{\Delta} = k_{De} \sqrt{2(u-c_s)/c_s} = k_{De} \sqrt{2(M-1)}. \quad (3)$$

Comparing Eq. (2) and (3), we get  $\Delta \approx 2/k_i$ , which means that the width of the soliton is determined by  $k_i$  in case of small amplitude solitons. Thus, in case of ion acoustic solitons, the dispersion relation determines not only the form of their tails but also their width.

Now, we extend this consideration to the case of an unmagnetized uniform plasma, the dispersion relation of which is written as,

$$\epsilon = \epsilon_0 \left( 1 - \frac{\omega_{pe}^2}{k^2 (u^2 - \gamma_e v_{te}^2)} - \frac{\omega_{pi}^2}{k^2 (u^2 - \gamma_i v_{ti}^2)} \right) = 0. \quad (4)$$

Here,  $\gamma_e$ ,  $\gamma_i$  and  $\omega_{pe}$  are specific heat ratios for electron and ion and electron plasma angular frequency, respectively.  $\gamma_{e,i}$  is 3 if  $u \gg v_{te,ti}$ , and is 1 if  $u \ll v_{te,ti}$ . When the phase velocity  $u$  is around the thermal velocity of electron and ion  $v_{te,ti}$ , the wave number  $k$  is a complex number and gives energy dissipation. The relation of  $u$  and  $k$  calculated from Eq. (4) is shown in Fig. 2. The regions of propagating electron waves and ion acoustic waves of real  $k$  appear when  $u > \sqrt{3}v_{te}$  and  $c_s > u > \sqrt{3}v_{ti}$ , respectively. On the other hand, the localized structures belong to the regions of non-oscillatory and propagating evanescent waves of imaginary  $k$ . Ion phase-space holes are able to propagate with a speed of  $u$  which is smaller than  $\sqrt{3}v_{ti}$ . Their tails of small perturbations must decay according to the

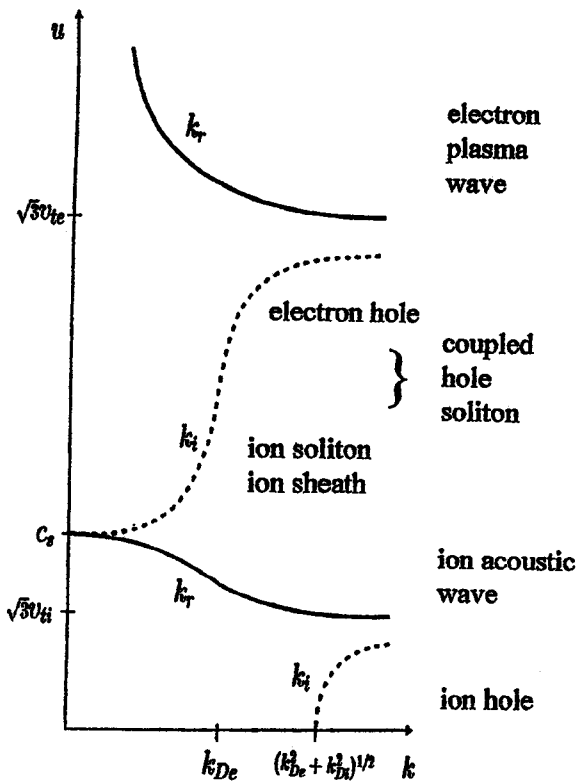


Fig. 2 The relation between phase-velocity  $u$  and wave number  $k$  in case of an unmagnetized uniform plasma. The figure shows the existence regions of an ion sheath and electron and ion holes, and suggests a new coupling state of an electron hole and an ion soliton (CHS).  $k_{Di}$  and  $k_{De}$  are wave numbers for electron and ion, respectively.

imaginary wave number  $k$  derived from the dispersion. In a like manner, ion acoustic solitons and ion sheaths exist when  $c_s < u$ , and electron phase-space holes exist when  $u < \sqrt{3}v_{te}$ . Thus, the region  $c_s < u < \sqrt{3}v_{te}$  includes ion solitons and electron holes, both of which have positive potential humps. Thus, this region suggests us a new localized structure being a coupled state of an electron phase-space holes and an ion acoustic solitons (CHS), which will be discussed in chapter 4.

### 3. Ion Phase-Space Hole

Ion phase-space holes belong to the region  $u < \sqrt{3}v_{ti}$  as shown in Fig. 2. The experiment has been performed in a double-plasma device which allows us to inject argon ions steadily or as a pulse into an argon target plasma. Typical plasma parameters are as follows; plasma density  $n_0 \sim 10^8 \text{ cm}^{-3}$ , electron temperature  $T_e \sim 2 - 3 \text{ eV}$  and ion temperature  $T_i \sim 0.2 - 0.3 \text{ eV}$ , with neutral-argon-gas pressure  $\sim (0.7 - 3) \times 10^{-4} \text{ Torr}$ . Thus, ion plasma frequency  $f_{pi} \sim 300 \text{ kHz}$ , and ion acoustic speed  $c_s \sim 3 \times 10^5 \text{ cm/sec}$ . An energy analyzer is used to detect the temporal behavior of ion energy. The obtained ion distribution function is displayed on a phase space of energy and time.

The temporal evolution of a plasma penetrated by a pulsed ion beam (pulse width  $\sim 3/f_{pi}$ ) is shown in Fig. 3 with a beam injection voltage  $\phi_b$  as a parameter. Here, the intensity of brightness in Fig. 3 is derivative of energy-analyzer output with respect to retarding voltage, and means ion energy distribution function depending on energy  $mv^2/2 + e\phi$  and time  $T$ .  $m$ ,  $v_i$  and  $\phi$  are ion mass, ion velocity and plasma potential, respectively. The brightness changed sharply at a fixed value of energy distribution function. The beam injection voltage  $\phi_b$  is varied up to 8 V. When  $\phi_b = 0.5 \text{ V}$ , we have a normal soliton signal on the phase space of energy and time. The hole is formed on the phase space when  $\phi_b = 1.5 \text{ V}$ , which injects a pulsed ion beam with a velocity faster than the ion acoustic speed  $c_s$ . Each ion hole propagates with a constant velocity. The hole size and the hole speed get large as  $\phi_b$  increases. The hole length varies within the extent of 0.5–1 cm, and the hole speed is  $(1.7-2) \times 10^5 \text{ cm/sec}$ . The too high  $\phi_b$  gives a burst formation accompanied by a broad density depression and induces no hole formation. Higher pulse voltage  $\phi_b$  excites a hole of a higher speed. Thus, we can excite two holes with different velocities. The coalescence of two holes into one large hole are also observed in phase space. An ion hole is incompressible in phase space in a collisionless plasma and behaves as a macroparticle.

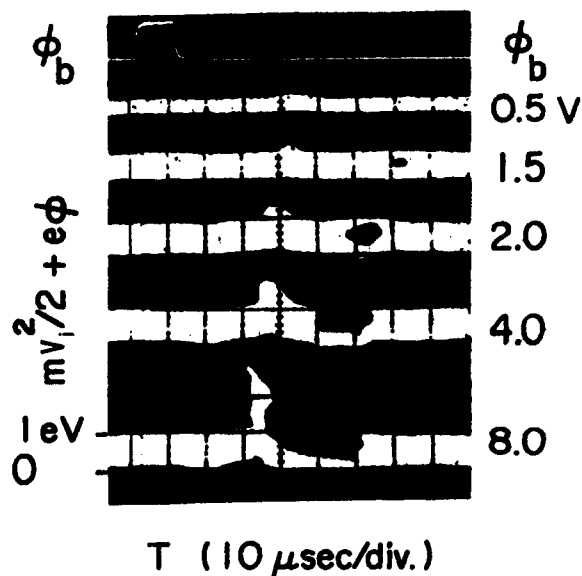


Fig. 3 Hole excitation by pulse injection of ion beam. Application of small pulse excites a normal ion soliton. Pulse voltages more than 1.5 V accelerate ions to the same order of ion acoustic speed and excite ion holes. Too big pulse voltages lead to no excitation.

Ions surrounding an ion hole are pulled by another ion hole of negative potential. Two ion holes accordingly attract each other like negative mass particles and unite into one hole. Thus, an ion hole is regarded as a negatively charged macroparticle with negative mass.

#### 4. Coupled Electron Hole and Ion Acoustic Soliton

The region  $c_s < u < \sqrt{3}v_{te}$  in Fig. 2 suggests the existence of a coupled state between an electron hole and an ion soliton. We adopt the electrostatic simulation of particle-in-cell (PIC) model with one dimensional coordinate  $x$  to find such a coupled state. In the case of immovable ions (mass ratio of ion to electron  $m_i/m_e = \infty$ ), an excited electron hole with a propagation velocity  $u = 0$  is very stable in phase space. On the other hand, the stability of this electron hole in the case of movable ions ( $m_i/m_e = 100$ ) is shown in Fig. 4, where the spatial structures of the normalized plasma potential  $e\phi/kT_e$ , the electron phase fluid in phase space ( $x/\lambda_D, v_e/v_{te}$ ) and the ion phase fluid in phase space ( $x/\lambda_D, v_i/c_s$ ) are demonstrated. Here,  $v_{te} = \sqrt{\kappa T_e/m_e}$ ,  $v_e$  and  $\lambda_D$  are electron velocity and electron Debye length, respectively.  $v_i$  is ion velocity, and  $c_s = \sqrt{\kappa T_e/m_i}$  is ion acoustic speed.  $T = \omega_{pe}t/2\pi$  is normalized time. The system length is  $125\lambda_D$  and consists of 3000 cells. Each

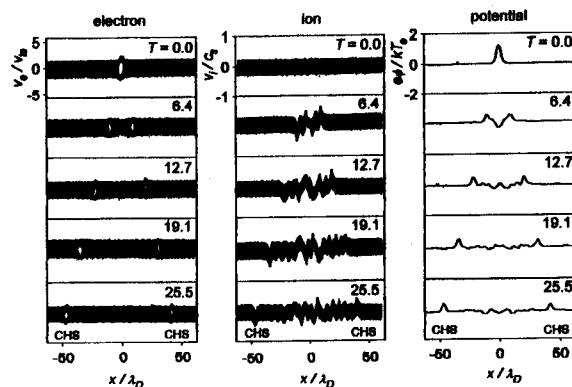


Fig. 4 Electron hole disruption and formation of coupled hole solitons CHSs observed in phase space ( $x/\lambda_D, v_e/v_{te}$ ), in phase space ( $x/\lambda_D, v_i/c_s$ ), and as spatial potential variation  $e\phi/kT_e$ .  $m_i/m_e = 100$ .  $T = \omega_{pe}t/2\pi$  is normalized time.

number of ions and electrons per unit cell is 1000. The temperature ratio of electron to ion  $T_e/T_i$  is 40 [9].

The positive potential of the electron hole causes the compression of ions on both sides of the hole. The resultant ion perturbations deform the hole itself and disrupt the hole into two holes. Apparently these two holes propagating in opposite directions to each other are accompanied by compressional ion pulses and form new solitary structures propagating stably. Each structure comprises an electron hole and an ion acoustic soliton, being regarded as a coupled state of an electron hole and an ion acoustic soliton, a coupled hole-soliton (CHS). The disruption mechanism for an electron hole is as follows. Each compressional ion pulse induced on both sides by the positive potential of the initial electron hole has also a positive potential. This positive potential of each ion pulse pulls the electrons surrounding the hole from both sides of it. In other words, the electron hole behaves as a macro particle having positive charge and negative mass [2], thereby being dragged by the positive potential of each ion pulse. As a result, the hole is elongated and divided into two holes. This drag is also the mechanism to maintain the stability of the CHS, where the positive potential of the ion acoustic soliton attaches the electron hole to the soliton.

We try to derive the theoretical relation between Mach number  $M = u/c_s$  and the maximum potential  $\Phi_{\max} = e\phi/kT_e$  of CHSs, according to ref. [8]. The spatial structure of a CHS in the moving frame of a CHS propagation velocity  $u$  is illustrated in Fig. 5. For simplicity, we assume a rectangular velocity distribution function of electrons; its spread and height are  $2v_{te}$  and

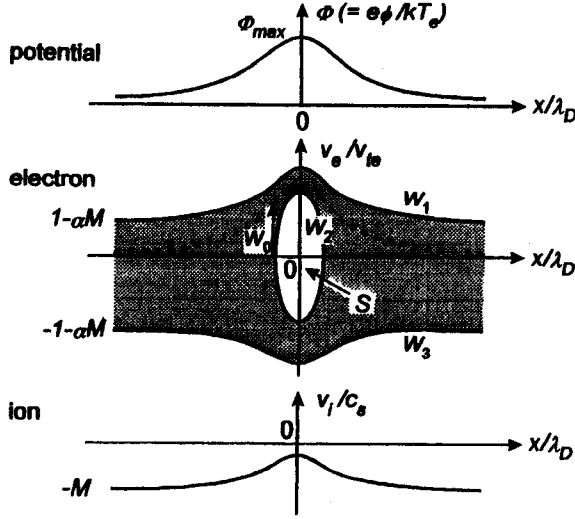


Fig. 5 Spatial structure of a coupled hole-soliton CHS (a coupled state of an electron hole and an ion acoustic soliton) with a propagation speed  $u$  under the water bag model. Upper, middle and lower figures indicate potential, electron phase fluid and ion phase fluid, respectively.  $M = u/c_s$ ,  $\Phi_{\max} = e\phi_{\max}/kT_e$ ,  $\alpha = (m_e/m_i)^{1/2}$ , and  $W_{0,1,2,3} = v_{0,1,2,3}/v_{te}$ .

$1/2v_{te}$  at  $x = \pm\infty$ , respectively.

$$f_e(v_e, x = \pm\infty) = \begin{cases} 1/2v_{te} & (-v_{te} - u \leq v_e \leq v_{te} - u) \\ 0 & (v_e \leq -v_{te} - u, v_{te} - u \leq v_e) \end{cases}$$

Thus, we are able to calculate the spatial electron density variation  $n_e(x)$  as a function of  $\phi(x)$  from the electron velocities on the boundaries of the electron phase fluid  $v_1$ ,  $v_2$  and  $v_3$ , being the velocities on upper, hole and lower boundaries of the electron phase fluid, respectively.

$$n_e(x) = n_0 \frac{v_1 + |v_3| - 2|v_2| \theta(v_2^2)}{2v_{te}}$$

Here,  $n_0$  is the plasma density at  $x = \pm\infty$ , and  $\theta(x)$  is step function.  $v_1$ ,  $v_2$ ,  $v_3$  are derived as a function of  $\phi(x)$  from the following energy equations,

$$\begin{aligned} v_{0,1,2,3} &= v_{te} W_{0,1,2,3} \\ \frac{1}{2} m_e (v_{te} - u)^2 &= \frac{1}{2} m_e v_1^2 - e\phi, \\ -\frac{1}{2} m_e v_0^2 &= \frac{1}{2} m_e v_2^2 - e\phi, \\ \frac{1}{2} m_e (-v_{te} - u)^2 &= \frac{1}{2} m_e v_3^2 - e\phi. \end{aligned}$$

$v_0$  is the velocity  $v_e$  of the electrons at  $v_2 = 0$  that have no kinetic energy ( $v_e = 0$ ) at  $x = \pm\infty$ . The ion temperature is assumed to be zero. Therefore, the spatial dependence of ion density  $n_i(x)$  as a function of  $\phi(x)$  is also calculated from the following conservation equations of ion energy and ion flux,

$$\begin{aligned} \frac{1}{2} m_i (-u)^2 &= \frac{1}{2} m_e v_i^2 - e\phi, \\ n_0 (-u) &= n_i v_i. \end{aligned}$$

Poisson's equation,  $\partial^2 \phi(x)/\partial x^2 = e(n_e(x) - n_i(x))/\epsilon_0$ , relates  $\phi(x)$  to  $n_i(x)$  and  $n_e(x)$ . Normalizing the quantities as  $z = x/\lambda_D$ ,  $\Phi = e\phi/kT_e$ , and  $W_0 = v_0/v_{te}$ , we obtain the following equation,

$$\begin{aligned} \frac{\partial^2 \Phi}{\partial z^2} &= \frac{1}{2} \left\{ \left[ (1 - \alpha M)^2 + 2\Phi \right]^{1/2} + \left[ (1 + \alpha M)^2 + 2\Phi \right]^{1/2} \right\} \\ &\quad - \theta(-W_0^2 + 2\Phi) \left[ -W_0^2 + 2\Phi \right]^{1/2} \\ &\quad - M(M^2 - 2\Phi)^{-1/2}. \end{aligned}$$

Here,  $z = x/\lambda_D$ ,  $\Phi = e\phi/kT_e$ ,  $W_0 = v_0/v_{te}$ ,  $\alpha = (m_e/m_i)^{1/2}$ . By integrating the above-mentioned equation multiplied by  $\partial\Phi/\partial z$  from  $-\infty$  to  $z$ , we derive Sagdeev's potential  $V(\Phi, M, W_0, \alpha)$  [10],

$$\begin{aligned} V(\Phi, M, W_0, \alpha) &= -\frac{1}{6} \left\{ \left[ (1 - \alpha M)^2 + 2\Phi \right]^{3/2} \right. \\ &\quad \left. + \left[ (1 + \alpha M)^2 + 2\Phi \right]^{3/2} - (1 - \alpha M)^3 - (1 + \alpha M)^3 \right\} \\ &\quad + \frac{1}{3} \theta(-W_0^2 + 2\Phi) \left[ -W_0^2 + 2\Phi \right]^{3/2} \\ &\quad + M \left[ M - (M^2 - 2\Phi)^{1/2} \right]. \end{aligned} \quad (5)$$

Here, Equation (5) is valid when  $\alpha M < 1$ , and we put  $V(0, M, W_0, \alpha) = 0$ .  $V(\Phi, M, W_0, \alpha)$  satisfies  $(1/2)(\partial\Phi/\partial z)^2 + V(0, M, W_0, \alpha) = 0$ . The CHS has a maximum potential  $\Phi_{\max}$  satisfying  $V(\Phi_{\max}, M, W_0, \alpha) = 0$ .

On the other hand, the hole area  $S$  of the CHS in the electron phase fluid is calculated as follows.

$$S = 4 \int_{\frac{W_0^2}{2}}^{\Phi_{\max}} \left( \frac{-W_0^2 + 2\Phi}{-2V(\Phi, M, W_0, \alpha)} \right)^{1/2} d\Phi. \quad (6)$$

Here,  $S$  is a function of  $\Phi_{\max}$ ,  $M$ ,  $W_0$ , and  $\alpha$ . Thus, by eliminating  $W_0$ , the equation  $V(\Phi_{\max}, M, W_0, \alpha) = 0$  and Eq. (6) yield the relation between  $M$  and  $\Phi_{\max}$  with  $S$  and  $\alpha$  as parameters. The theoretical  $M - \Phi_{\max}$  relation

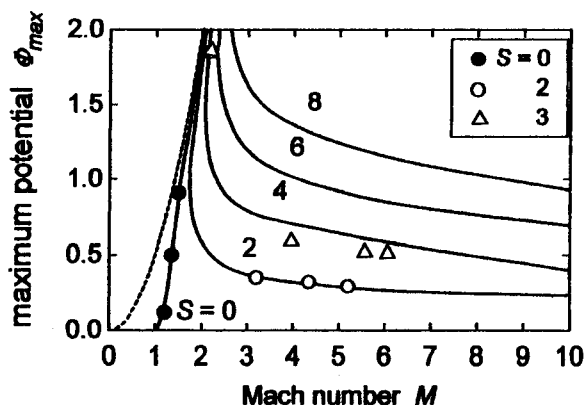


Fig. 6 Relation between the Mach number  $M$  and the maximum potential  $\Phi_{\max}$  of CHSs with hole area  $S$  in electron phase fluid as a parameter.  $\bullet$ ,  $\circ$  and  $\triangle$  are experimental points.  $m_i/m_e = 100$ . Here, CHSs of  $S = 0$  mean pure ion acoustic solitons, and the dotted line ( $\Phi = M^2/2$ ) indicates the critical line of ion reflection due to the CHS potential  $\phi$ .

of CHSs in the case of  $\alpha = 0.1$  ( $m_i/m_e = 100$ ) is plotted with  $S$  as a parameter on Fig. 6. The dotted line expresses  $\Phi = M^2/2$ , and means the critical line of ion reflection due to the positive potential of CHSs. When  $S$  becomes finite, the Mach number  $M$  of the CHS increases. The aspect (height-to-width) ratio of the elliptic hole in the electron phase fluid grows along the theoretical curve of  $S = \text{const.}$  with an increase in  $\Phi_{\max}$ . The large Mach number gives pure electron holes. Hence, Fig. 6 provides the unified description of pure ion acoustic solitons ( $S = 0$ ), coupled hole-solitons and pure electron holes ( $M \gg 1$ ). The theoretical curves well explain the experimental data.

## 5. Conclusions

- (1) The dispersion relation (the phase velocity  $u$  versus the wave number  $k$ ) suggests the possible region of existence for localized structures, where  $u$  is real and  $k$  is imaginary. The characteristic length of the tail of localized structures propagating with a speed  $u$  must be  $1/k_i$ .
- (2) In case of small-amplitude ion solitons,  $1/k_i$  means not only the characteristic length of the soliton tail but also a half of the soliton width.
- (3) From the dispersion relation of an unmagnetized uniform plasma, we can expect the existence of a localized structure coupling between an electron

hole and an ion soliton, in addition to an electron hole, an ion soliton, an ion sheath and an ion hole.

- (4) The phase-space observation of ion holes reveals their dynamics in phase-space. The pulse injection of ion beam causes rolling up the phase-space region of no ion and forms symmetric ion holes. The injected beam velocity  $v_b$  must be higher than the ion acoustic speed  $c_s$ . The excited ion holes are stable during their propagation.
- (5) An electron hole whose velocity  $u$  is slower enough than the electron thermal speed  $v_{te}$  interacts strongly with ions. The ion motion induced by the electron hole gives rise to the hole disruption into two or more holes.
- (6) The disrupted holes are coupled with the ion perturbations and form coupled states of electron holes and ion solitons (CHSs). These coupled hole solitons (CHSs) are stable during their propagation.

## References

- [1] H. Schamel, Phys. Reports **140**, 161 (1986).
- [2] H.L. Berk and K.V. Roberts, Phys. Fluids **10**, 1595 (1967); H.L. Berk, C.E. Nielsen and K.V. Roberts, Phys. Fluids **13**, 980 (1970).
- [3] K. Saeki, P. Michelsen, H.L. Pécseli and J.J. Rasmussen, Phys. Rev. Lett. **42**, 501 (1979).
- [4] H.L. Pécseli, R.J. Armstrong and J. Trulsen, Phys. Lett. **81A**, 386 (1981).
- [5] T. Sato and H. Okuda, Phys. Rev. Lett. **44**, 740 (1980).
- [6] H. Fujita, S. Yagura and K. Matsuo, Phys. Fluids **27**, 2948 (1984).
- [7] H. Matsumoto *et al.*, Geophys. Res. Lett. **21**, 2915 (1994). Their naming of electrostatic solitary waves gives confusion, because the hole is out of the wave category.
- [8] K. Saeki and J.J. Rasmussen, J. Phys. Soc. Japan **60**, 735 (1991).
- [9] K. Saeki and H. Genma, Physical Review Letters, **80**, 1224 (1998).
- [10] R.Z. Sagdeev, *Reviw of Plasma Physics*, Vol. 4 (New York, Consultants Bureau, ed. by M.A. Leontovich), p. 23 (1966).